La substitution studies on the heavy-fermion superconductor $CeRh_2As_2$

Sushma Lakshmi Ravi Sankar,[1,2] Manuel Brando,[1] Jochen Wosnitza,[2,3] and Seunghyun Khim[1,*]

[1]*Max Planck Institute for Chemical Physics of Solids, Nöthnitzer Straße 40, 01187 Dresden, Germany*

[2]*Institute for Solid State and Materials Physics, Technische Universität Dresden, 01062 Dresden, Germany*

[3]*Dresden High Magnetic Field Laboratory (HLD-EMFL) and Würzburg-Dresden Cluster of Excellence ctd.qmat, Helmholtz-Zentrum Dresden-Rossendorf, 01328 Dresden, Germany*

(Received 23 February 2026; revised 5 August 2026; accepted 7 August 2026; published 25 August 2026)

$CeRh_2As_2$ has been receiving considerable attention due to its unusual two-phase superconductivity. The superconducting (SC) phase appears at $T_c = 0.35$ K in an ordered state (phase I) of the Ce-4f moments, which develops below $T_0 = 0.55$ K. The microscopic nature of phase I has not been fully established yet. We report a single-crystal study of the effect of La substitution on these low-temperature phases in $Ce_{1-x}La_xRh_2As_2$ up to $x = 0.1$. The lattice parameters increase monotonically with x, corresponding to an effective negative pressure of approximately -0.3 GPa for $x = 0.1$. While the Ce^{3+} local valence state and the non-Fermi-liquid behavior are preserved, the resistivity coherence maximum $T^*_{max} \approx 45$ K in the pristine sample shifts to lower temperatures with increasing x, indicating a suppression of the Kondo energy scale upon lattice expansion. On the other hand, both T_c and T_0 are rapidly suppressed to below 0.1 K for $x > 0.05$. Notably, such a rapid decrease of T_c under moderate negative pressure is unexpected, but is rather consistent with a substitution-induced disorder effect which leads to strong pair breaking in unconventional superconductors. The observed fragility of phase I under both pressure and disorder may imply its itinerant origin.

DOI: 10.1103/f79y-ssdx

I. INTRODUCTION

$CeRh_2As_2$ is an intriguing heavy-fermion superconductor. Although its superconducting (SC) transition temperature is comparatively low, $T_c = 0.35$ K, the upper critical field (H_{c2}) for field aligned along the c axis is as high as 18 T [1]. This H_{c2} significantly exceeds the Pauli-limiting field of $H_P = 1.84T_c \approx 0.6$ T, which sets an upper limit for weak-coupling spin-singlet superconductivity, and thus strongly hints at possible spin-triplet pairing. Indeed, the SC phase diagram demonstrates a phase boundary within the SC state indicating a transition from a low-field even-parity (SC1) state to a high-field odd-parity (SC2) state [2]. This behavior has been attributed to the cooperation of heavy-fermion superconductivity and strong spin-orbit coupling that originates from the lack of local inversion symmetry at the Ce site in the centrosymmetric crystal structure [3–10]. Furthermore, the high-field SC2 phase is proposed to have nontrivial topology [11,12].

In addition, the Ce-4f moments order at $T_0 = 0.55$ K, forming a state, called phase I, whose microscopic nature has not been fully established yet [13]. While antiferromagnetism has been suggested by the presence of a spontaneous internal field detected below T_0 [14–16], this picture is challenged by experimental observations: An in-plane magnetic field enhances T_0, and further induces a cascade of new phases [17–20]. An alternative explanation involves a higher multipolar order of the Ce-4f moments. A quasiquartet crystal-electric field (CEF) ground state [21] combined with a Kondo energy scale comparable to the CEF splitting can stabilize quadrupole degrees of freedom despite being usually forbidden in tetragonal systems. Accordingly, several theoretical models have been proposed based on a local picture with cooperating dipole and multipolar orders [22,23] and an itinerant scenario involving Fermi-surface nesting [17].

The SC and phase I might be intimately linked in terms of quantum criticality. Nonthermal fluctuations, which arise as the ordered state is suppressed toward zero temperature, possibly mediate unconventional SC pairing. This is supported by a departure from Fermi-liquid behavior in both specific heat and resistivity, signaling strong electronic correlations and proximity to a quantum critical point (QCP) [24]. Thus, identifying the microscopic nature of the T_0 order will help illuminate the SC pairing mechanism as well as the origin of the multiple SC phases in $CeRh_2As_2$ [25–27].

Strong electronic correlations, as evidenced by the quantum-critical behavior and the small energy scales associated with the ordered phases, imply that the fundamental properties of $CeRh_2As_2$ are highly sensitive to external parameters. By systematically tuning the external parameters such as pressure, magnetic field, and compositions, one can associate physical quantities with underlying microscopic interactions. Recent studies demonstrated a tunability of the SC

*Contact author: seunghyun.khim@cpfs.mpg.de

Published by the American Physical Society under the terms of the Creative Commons Attribution 4.0 International license. Further distribution of this work must maintain attribution to the author(s) and the published article's title, journal citation, and DOI. Open access publication funded by Max Planck Society.

and phase I under hydrostatic pressures [28–30]. A QCP was revealed at $P_c = 0.5$ GPa, where T_0 is almost suppressed, T_c is maximized, and a T-linear resistivity becomes most pronounced [30]. This indicates an intimate connection between superconductivity and the ordering of the Ce-4f moments.

In the present work, we have characterized La-substituted $CeRh_2As_2$ single crystals to probe the nature of the low-temperature phases through nonmagnetic substitution on the Ce site. While La substitution up to 10% preserves the local Ce^{3+} valence state and the non-Fermi-liquid behavior observed in the pristine compound, it induces a monotonic expansion of the unit-cell volume. This lattice expansion, corresponding to an effective negative pressure, likely shifts the local resistivity maximum toward lower temperatures by reducing the Kondo energy scale. However, the rapid suppression of both T_c and T_0 with increasing La concentration suggests that the concomitant disorder effect dominates over the pressure effect. We discuss how these observations provide insights into the unconventional SC gap structure and the itinerant nature of phase I.

II. EXPERIMENT

We have grown single crystals of $Ce_{1-x}La_xRh_2As_2$ ($x = 0.01$, 0.03, 0.04, 0.05, and 0.1, where x denotes the nominal concentration of La) using the bismuth (Bi) flux-growth method [1,18]. Powder x-ray diffraction (PXRD) measurements were used to confirm the phase purity and to characterize the crystal structure. To endure accurate determination of the lattice parameters, LaB_6 was used as a standard [31]. The chemical compositions of the crystals were determined by using energy dispersive x-ray spectroscopy (EDX). The measurements were performed on at least five distinct spots across the sample surface, which confirms uniform distribution of the elemental composition. Magnetization and specific-heat measurements were performed in a quantum design magnetic property measurement system (MPMS) and physical property measurement system (PPMS), respectively. Electrical resistivity was measured using the standard four-probe method in the PPMS. Low-temperature resistivity characterizations below 1.8 K were obtained by using a customized adiabatic demagnetization refrigeration probe in the PPMS.

III. RESULTS

A. Crystal structure and chemical composition

PXRD measurements combined with Rietveld refinement confirmed that the $Ce_{1-x}La_xRh_2As_2$ single crystals crystallize in the $CaBe_2Ge_2$-type structure, identical to that of the pristine compound [3]. No additional diffraction peaks were observed, indicating the absence of secondary phases. The actual La composition determined by EDX (x_{EDX}) is systematically higher than the nominal value x by a factor of approximately 1.4 ($x_{EDX} = 0.0404 \pm 0.0035$, 0.0633 ± 0.0024, and 0.145 ± 0.0022 for $x = 0.03$, 0.5, and 0.1, respectively). For $x < 0.03$, the La concentration is below the instrumental detection limit of EDX.

The lattice parameters determined using the LaB_6 standard are shown in Fig. 1. Both the a and c lattice parameters

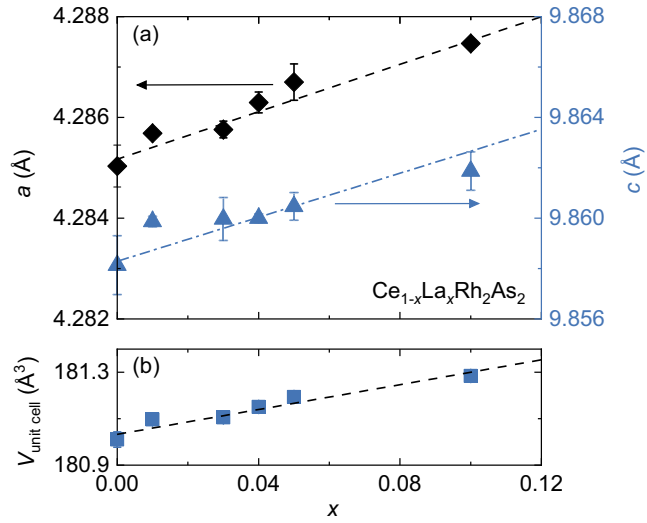


FIG. 1. La-concentration (x) dependence of (a) the tetragonal unit-cell lattice parameters, a and c, and (b) the calculated unit-cell volume, $V_{\text{unit cell}}$.

monotonically increase with increasing x, following Vegard's law. This behavior is consistent with the larger atomic radius of La (187 pm) compared to Ce (181 pm), leading to a systematic lattice expansion upon substitution. For $x = 0.1$, the a and c lattice parameters increase by 0.057% and 0.038%, respectively, resulting in a total unit-cell volume increase of approximately 0.15%. An increase of the unit-cell volume by La substitution has also been observed in other Ce-based heavy-fermion superconductors, such as $CePt_2Si_2$ [32], $CeCu_2Si_2$ [33–35], and $CeCoIn_5$ [36]. In contrast to the relatively isotropic expansion observed in $CeRh_2As_2$, the isomorphic (Ce, La)Cu_2Si_2 system in the $ThCr_2Si_2$-type structure exhibits a pronounced increase in the a parameter with minimal change in the c parameter [35]. The $CaBe_2Ge_2$-type structure features a strong bonding along the c axis, particularly between Rh(2) and As(2), with a Ce atom positioned intermediately [32,37]. The substitution of Ce with La will directly disturb the Rh(2)-As(2) bonding, rendering a more significant expansion along the c axis.

B. Magnetization

Figure 2 depicts the temperature-dependent inverse magnetic susceptibility data of the $x = 0.1$ sample, the highest La concentration studied. To access the impact of the La substitution on the local magnetic state of Ce, we focus on this sample representing the most significant chemical perturbation in our compounds studied. Above 100 K, the linear slopes of the Curie-Weiss behavior are seen for both field directions. The effective moment, determined by using the high-temperature fits, is close to $2.56\mu_B$/Ce for the Ce^{3+} valence state. No significant change of χ is observed in the $x = 0.1$ sample compared to the pristine $CeRh_2As_2$. From the high-temperature Curie-Weiss fit, the Curie-temperature was obtained to be $\theta_{ab} = 24.8$ K and $\theta_c = 82.8$ K. The estimated B_2^0 parameter in the Hamiltonian describing the CEF model is 6.04 K. This value is slightly smaller than $B_2^0 = 6.5$ K of the

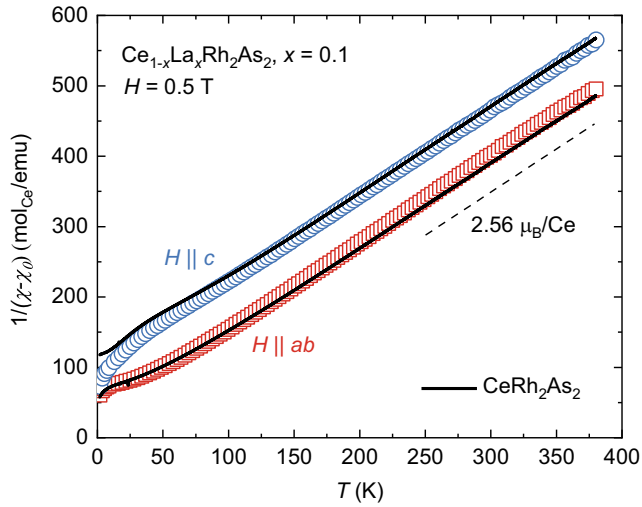


FIG. 2. Temperature dependence of the inverse magnetic susceptibility (χ) after subtracting a temperature-independent term (χ_0) for in-plane ($H \parallel ab$, red open squares) and c-axis ($H \parallel c$, blue open circles) magnetic fields, respectively. The magnetic susceptibility per Ce is obtained by normalization using the x_{EDX} value. The solid lines denote the magnetic-susceptibility data of pristine $CeRh_2As_2$, reported earlier [1]. The slope of the linear dashed line stands for $2.56\mu_B$/Ce, which is the expected effective moment of the Ce^{3+} valence state.

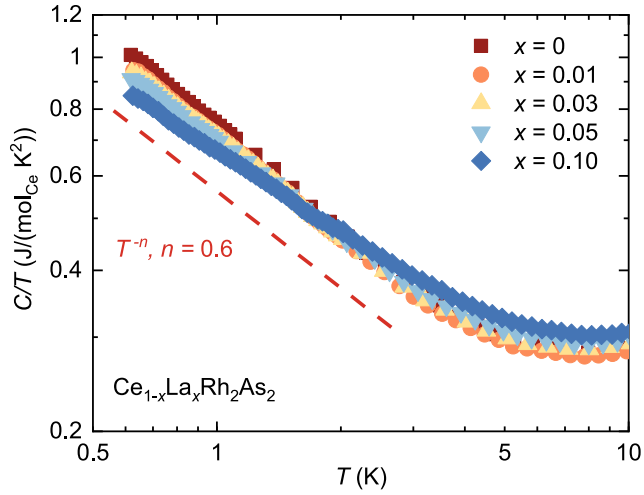


FIG. 3. Specific heat divided by temperature for different La concentrations, x. C/T was normalized by the Ce concentration determined by EDX ($1 - x_{\mathrm{edx}}$).

pristine $CeRh_2As_2$ [1]. However, by applying the same value of $B_4^0 = 0.1$ K and $B_4^4 = 2.8$ K used for $CeRh_2As_2$, we could also obtain a fairly good fit (see Supplemental Material [38]). This supports the assumption that the local Ce state is intact up to $x = 0.1$, allowing us to consider the substitution to be perturbative. A more pronounced Curie-Weiss tail is observed for $H \parallel c$ (blue open circles in Fig. 2) at low temperatures, appearing as a sharper drop in $1/\chi$. This anomaly may indicate the presence of paramagnetic impurities, possibly introduced by the chemical substitution [38].

C. Specific heat

Figure 3 shows the temperature dependence of the specific heat divided by temperature, C/T, for various x. Since the La substitution is expected to minimally affect the lattice-phonon contribution, the observed evolution of C/T with x primarily reflects changes in the electronic and magnetic specific heat. The power-law increase of $C/T \propto T^{-n}$ upon cooling persists even at $x = 0.1$, indicating the continued presence of quantum critical fluctuations. However the C/T value at low temperatures gradually decreases with increasing x, and the exponent n is systematically reduced. This trend reflects a weakening of electronic correlations and a suppression of quantum critical fluctuations. The reduced C/T below 2 K is compensated by a concomitant increase in C/T at higher temperatures, suggesting a redistribution of the magnetic entropy while maintaining the quasiquartet CEF ground state [1,17,21]. Further quantitative analysis remains to be done in specific-heat characterizations at even lower temperatures.

D. Resistivity

Figure 4 displays the normalized temperature-dependent resistivity, $\rho(T)/\rho_{300\,\mathrm{K}}$. We note that the room-temperature resistivity value ($\rho_{300\,\mathrm{K}}$) does not monotonically increase with x, probably due to extrinsic factors such as cracks within the sample or uncertainties in determining the sample geometry. While the normalized resistivities above 50 K are almost identical across all x, $\rho/\rho_{300\,\mathrm{K}}$ systematically increases with x below the local maximum at T^*_{max}, evidencing increased disorder and disruption of the Kondo coherence. As a result, T^*_{max} decreases from 45 K for $x = 0$ to 40 K for $x = 0.1$ [Fig. 4(b)].

At lower temperatures, both T_c and T_0 are reduced with increasing x. Above $x = 0.03$, the zero-resistivity transition becomes undetectable, as T_c is suppressed below 0.12 K, the lowest temperature accessible in our experiments. Similarly, T_0 shifts to lower temperatures and disappears for $x > 0.05$. The suppression rates, given by the slopes of the T_c and T_0 changes, are -5.9 K/x and -4.8 K/x, respectively.

IV. DISCUSSION

The main experimental findings can be summarized as follows: (1) Partial substitution of Ce atoms with La induces a systematic lattice expansion in $CeRh_2As_2$. (2) Simultaneously, it introduces additional disorder. (3) The local moment of the Ce^{3+} ($4f^1$) remains intact up to $x = 0.1$, together with persisting non-Fermi-liquid behavior as observed in pristine $CeRh_2As_2$. (4) While T^*_{max} decreases moderately, both T_c and T_0 are rapidly suppressed with increasing x. The observation (3) indicates that the La substitution can be considered as a perturbative tuning parameter rather than a fundamental change to the electronic structure. This will allow us to interpret the changes in the low-temperature properties (4) as combined consequences of two effects: (1) the effective negative pressure from the lattice expansion and (2) additional disorder induced by chemical substitution.

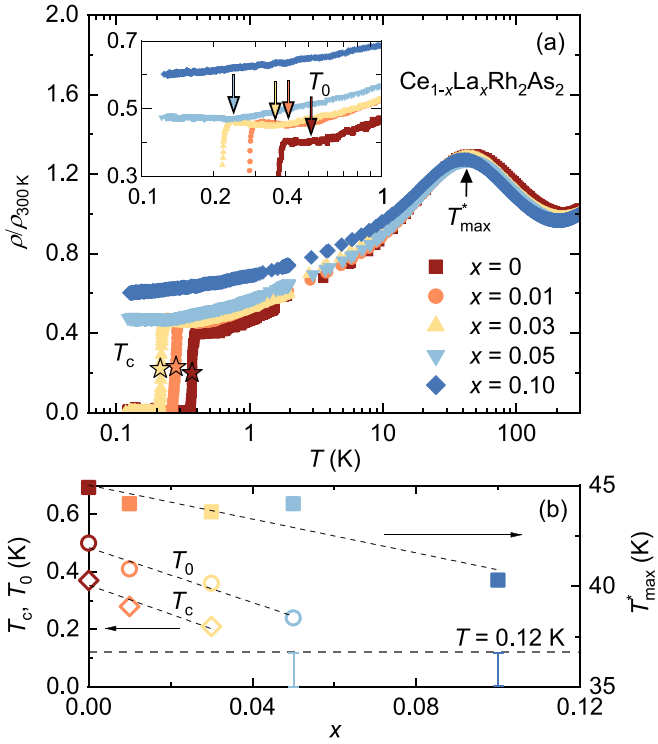


FIG. 4. (a) Temperature dependence of the normalized resistivity $\rho/\rho_{300\,K}$ for $Ce_{1-x}La_xRh_2As_2$. The T_c and T_0 transition temperatures are marked in the main panel and in the inset, respectively. T_c is determined as the midpoint of the zero-resistivity transition. T_0 is identified as the temperature at the onset of the resistivity upturn, which corresponds to the maximum in the second derivative of the resistivity. A detailed description is provided in the Supplemental Material [38]. (b) T_0 (open circles), T_c (open diamonds), and T^*_{max} (solid squares) as a function of nominal La composition x. The light blue and dark blue error bars indicate the possibility of T_c and T_0 transition temperatures, respectively, below 0.12 K.

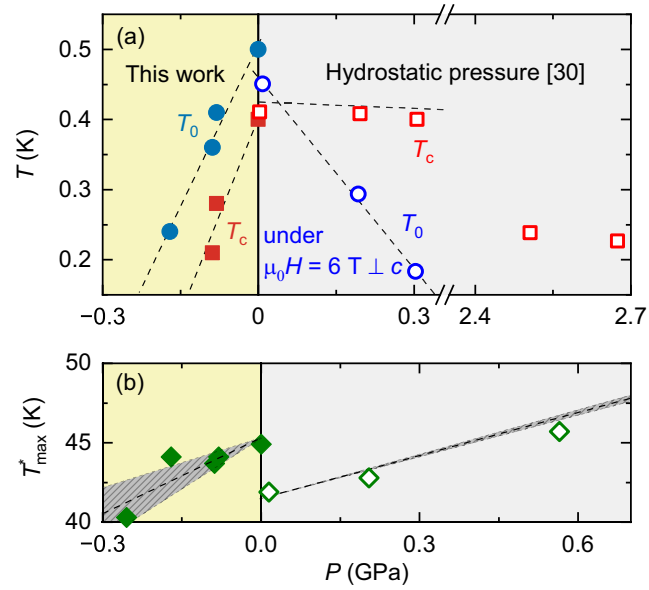


FIG. 5. Phase diagrams with respect to pressure for (a) T_c and T_0 and (b) T^*_{max}. The gray-shaded region in (b) represents the uncertainty in the rate of change of T^*_{max} with respect to pressure. The T_0 transition under hydrostatic pressure [30] was determined under an applied in-plane magnetic field of 6 T to observe the transition temperature by suppressing superconductivity. Since the T_0 transition is insensitive to in-plane magnetic field in this field scale, this result should represent the zero-field properties of T_0.

To disentangle the effect of the lattice expansion from that of additional disorder on the transition temperatures of T_c, T_0, and T^*_{max}, we compare our results with previous hydrostatic-pressure studies [30], treating La substitution as an extension to the negative pressure regime. Neglecting the slightly anisotropic lattice expansion, the effective hydrostatic pressure for each La concentration can be estimated from the change in the unit-cell volume based on the theoretical value of the bulk modulus, $B = 168$ GPa [39]. This estimates the unit-cell expansion for the $x = 0.1$ substitution ($\Delta V_{unit\ cell} \approx 0.15\%$) to correspond to about -0.25 GPa. The combined phase diagrams are shown in Fig. 5.

As shown in Fig. 5(b), T^*_{max} continuously increases as the lattice shrinks in the overall pressure range. The dashed line on the right panel represents the guide passing through the pressure-study data measured up to 2.69 GPa [30]. This behavior is consistent with the expectation that a compression of the Kondo lattice strengthens the Kondo exchange interaction. The discrepancy of the T^*_{max} values at zero pressure may arise from a slight quality difference between the two independent samples used in the experiments. The rate of the change of T^*_{max} can be larger on the negative side (15.9 ± 5.5 K/GPa) than on the positive side (9.0 ± 0.3 K/GPa). Although the size of the slope difference is still within the experimental error, the possible stronger suppression of T^*_{max} for negative pressures can be attributed to additional disorder effects.

On the other hand, T_c and T_0, shown in Fig. 5(a), demonstrate a contrasting pressure-dependent behavior on the positive and negative side. While T_c quickly vanishes and is no longer resolvable below ~ -0.2 GPa, it remains relatively robust under positive pressure. In contrast, T_0 is suppressed over a narrow range of pressure in both regimes. Given that T_c and T_0 are expected to be enhanced by increasing effective negative pressure, based on their behavior found under positive pressure, the observed suppression upon substitution cannot be explained by lattice expansion alone. These findings indicate that the primary origin of the changes in T_c and T_0 is disorder introduced by substitution, rather than the hydrostatic pressure effect.

The rapid suppression of T_c in $CeRh_2As_2$ is indicative of unconventional superconducting pairing. Heavy-fermion superconductivity mediated by magnetic fluctuations is typically characterized by strongly anisotropic gap structures with a sign change of the order parameter, rendering it to be highly sensitive to impurity scattering. In Fig. 6, we compare the normalized T_c under La substitution of $CeRh_2As_2$ with other Ce-based heavy-fermion superconductors, $CeCoIn_5$ [36] and $CeCu_{2.2}Si_2$ [40]. Overall, La substitution reduces T_c by at least a factor of 2 at $x = 0.1$. The differences in the relative T_c reduction reflect variations in underlying microscopic parameters [41]. While the Abrikosov-Gorkov model applied to our experimental data might associate the reduction of T_c with an anisotropic gap symmetry [42,43], we could not draw a

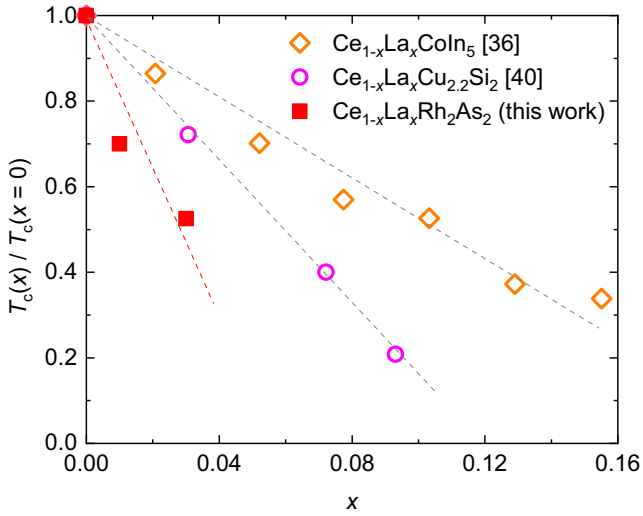


FIG. 6. Evolution of the normalized T_c, T_c/T_c $(x = 0)$, with respect to La concentration, x, in $CeCoIn_5$ [36], $CeCu_{2.2}Si_2$ [40], and $CeRh_2As_2$ (this work).

reasonable conclusion. A detailed analysis is provided in the Supplemental Material [38]. Nevertheless, superconductivity in $CeRh_2As_2$ appears to be the most sensitive among the three systems [38]. Here, we consider the unique structural character of $CeRh_2As_2$ to be potentially responsible for the particular vulnerable nature of T_c. As mentioned earlier, the lack of inversion symmetry on the Ce site introduces sublattice degrees of freedom that are involved in the SC order parameter [10]. The requirement for such spatial pairwise coherence which is essential for maintaining superconductivity could make the system more susceptible to local disorder than the other Ce-based superconductors. This additional pair-breaking mechanism will be independent from the one given by an anisotropic gap structure, which may explain the more rapid T_c suppression upon La substitution in $CeRh_2As_2$.

Finally, we turn to the evolution of T_0 under hydrostatic pressure and La substitution. Since hydrostatic pressure suppresses T_0 upon lattice compression, one could naively expect that the negative effective pressure given by La substitution could instead enhance T_0. However, our result shows a decrease in T_0 upon lattice expansion, even at a similar rate in terms of effective pressure. This suggests that the T_0 suppression by La substitution is primarily caused by a disorder effect. The destabilization of phase I upon both disorder and lattice change may support the proposed itinerant origin of the phase [17,44–47], driven by Fermi-surface nesting. In such a scenario, the nesting condition is highly sensitive to a change in the Fermi-surface geometry (by hydrostatic pressure) and a reduction of coherent scattering between the nested part of the Fermi surface (by substitution).

To summarize, we have investigated La-substituted $CeRh_2As_2$ single crystals up to $x = 0.1$. Substitution of Ce with La induces a systematic increase of the a and c lattice parameters without significantly altering the local Ce^{3+} valence state. The resulting negative effective pressure is reflected in a gradual decrease of the local resistivity maximum, T^*_{max}, consistent with the reduction of the Kondo-energy scale upon lattice expansion. However, the rapid suppression of both the SC and phase I is attributed to the dominant role of disorder induced by substitution. These findings can be related to the unconventional pairing nature of superconductivity and the itinerant origin of phase I.

ACKNOWLEDGMENTS

S.L.R.S. and S.K. were supported by the Max Planck Society and the Deutsche Forschungsgemeinschaft (DFG) - KH 387/1-1. J.W. acknowledges support from DFG through the Würzburg-Dresden Cluster of Excellence on Complexity, Topology and Dynamics in Quantum Matter–*ctd.qmat* (EXC 2147, Project No. 390858490), as well as the support of the HLD at HZDR, member of the European Magnetic Field Laboratory (EMFL).

DATA AVAILABILITY

The data that support the findings of this article are openly available [48].

[1] S. Khim, J. F. Landaeta, J. Banda, N. Bannor, M. Brando, P. M. R. Brydon, D. Hafner, R. Küchler, R. Cardoso-Gil, U. Stockert, A. P. Mackenzie, D. F. Agterberg, C. Geibel, and E. Hassinger, Field-induced transition from even to odd parity superconductivity in $CeRh_2As_2$, Science **373**, 1012 (2021).

[2] J. F. Landaeta, P. Khanenko, D. C. Cavanagh, C. Geibel, S. Khim, S. Mishra, I. Sheikin, P. M. R. Brydon, D. F. Agterberg, M. Brando, and E. Hassinger, Field-angle dependence reveals odd-parity superconductivity in $CeRh_2As_2$, Phys. Rev. X **12**, 031001 (2022).

[3] R. Madar, P. Chaudouet, J. Senateur, S. Zemni, and D. Tranqui, New ternary pnictides with the $CaBe_2Ge_2$-type structure in the systems, rare-earth-Rh-P and rare-earth-Rh-As, J. Less-Common Met. **133**, 303 (1987).

[4] T. Yoshida, M. Sigrist, and Y. Yanase, Pair-density wave states through spin-orbit coupling in multilayer superconductors, Phys. Rev. B **86**, 134514 (2012).

[5] D. Maruyama, M. Sigrist, and Y. Yanase, Locally noncentrosymmetric superconductivity in multilayer systems, J. Phys. Soc. Jpn. **81**, 034702 (2012).

[6] M. Sigrist, D. F. Agterberg, M. H. Fischer, J. Goryo, F. Loder, S.-H. Rhim, D. Maruyama, Y. Yanase, T. Yoshida, and S. J. Youn, Superconductors with staggered noncentrosymmetricity, J. Phys. Soc. Jpn. **83**, 061014 (2014).

[7] E. G. Schertenleib, M. H. Fischer, and M. Sigrist, Unusual H-T phase diagram of $CeRh_2As_2$: The role of staggered noncentrosymmetricity, Phys. Rev. Res. **3**, 023179 (2021).

[8] D. Möckli and A. Ramires, Two scenarios for superconductivity in $CeRh_2As_2$, Phys. Rev. Res. **3**, 023204 (2021).

[9] D. C. Cavanagh, T. Shishidou, M. Weinert, P. M. R. Brydon, and D. F. Agterberg, Nonsymmorphic symmetry and field-driven odd-parity pairing in $CeRh_2As_2$, Phys. Rev. B **105**, L020505 (2022).

[10] M. H. Fischer, M. Sigrist, D. F. Agterberg, and Y. Yanase, Superconductivity and local inversion-symmetry breaking, Annu. Rev. Condens. Matter Phys. **14**, 153 (2023).

[11] K. Nogaki, A. Daido, J. Ishizuka, and Y. Yanase, Topological crystalline superconductivity in locally noncentrosymmetric $CeRh_2As_2$, Phys. Rev. Res. **3**, L032071 (2021).

[12] J. Ishizuka, K. Nogaki, M. Sigrist, and Y. Yanase, Correlation-induced Fermi surface evolution and topological crystalline superconductivity in $CeRh_2As_2$, Phys. Rev. B **110**, L140505 (2024).

[13] G. Chajewski and D. Kaczorowski, Discovery of magnetic phase transitions in heavy-fermion superconductor $CeRh_2As_2$, Phys. Rev. Lett. **132**, 076504 (2024).

[14] M. Kibune, S. Kitagawa, K. Kinjo, S. Ogata, M. Manago, T. Taniguchi, K. Ishida, M. Brando, E. Hassinger, H. Rosner, C. Geibel, and S. Khim, Observation of antiferromagnetic order as odd-parity multipoles inside the superconducting phase in $CeRh_2As_2$, Phys. Rev. Lett. **128**, 057002 (2022).

[15] S. Ogata, S. Kitagawa, K. Kinjo, K. Ishida, M. Brando, E. Hassinger, C. Geibel, and S. Khim, Parity transition of spin-singlet superconductivity using sublattice degrees of freedom, Phys. Rev. Lett. **130**, 166001 (2023).

[16] S. Khim, O. Stockert, M. Brando, C. Geibel, C. Baines, T. J. Hicken, H. Luetkens, D. Das, T. Shiroka, Z. Guguchia, and R. Scheuermann, Coexistence of local magnetism and superconductivity in the heavy-fermion compound $CeRh_2As_2$ revealed by μSR studies, Phys. Rev. B **111**, 115134 (2025).

[17] D. Hafner, P. Khanenko, E.-O. Eljaouhari, R. Küchler, J. Banda, N. Bannor, T. Lühmann, J. F. Landaeta, S. Mishra, I. Sheikin, E. Hassinger, S. Khim, C. Geibel, G. Zwicknagl, and M. Brando, Possible quadrupole density wave in the superconducting Kondo lattice $CeRh_2As_2$, Phys. Rev. X **12**, 011023 (2022).

[18] K. Semeniuk, D. Hafner, P. Khanenko, T. Lühmann, J. Banda, J. F. Landaeta, C. Geibel, S. Khim, E. Hassinger, and M. Brando, Decoupling multiphase superconductivity from normal state ordering in $CeRh_2As_2$, Phys. Rev. B **107**, L220504 (2023).

[19] J. Bławat, G. Chajewski, D. Gnida, J. Singleton, O. Ayala Valenzuela, D. Kaczorowski, and R. D. McDonald, Competing electronic ground states in the heavy-fermion superconductor $CeRh_2As_2$, Phys. Rev. X **15**, 041057 (2025).

[20] P. Khanenko, J. F. Landaeta, S. Ruet, T. Lühmann, K. Semeniuk, M. Pelly, A. W. Rost, G. Chajewski, D. Kaczorowski, C. Geibel, S. Khim, E. Hassinger, and M. Brando, Phase diagram of $CeRh_2As_2$ for out-of-plane magnetic field, Phys. Rev. B **112**, L060501 (2025).

[21] D. S. Christovam, M. Ferreira-Carvalho, A. Marino, M. Sundermann, D. Takegami, A. Melendez-Sans, K. D. Tsuei, Z. Hu, S. Rößler, M. Valvidares, M. W. Haverkort, Y. Liu, E. D. Bauer, L. H. Tjeng, G. Zwicknagl, and A. Severing, Spectroscopic evidence of Kondo-induced quasiquartet in $CeRh_2As_2$, Phys. Rev. Lett. **132**, 046401 (2024).

[22] B. Schmidt and P. Thalmeier, Anisotropic magnetic and quadrupolar H-T phase diagram of $CeRh_2As_2$, Phys. Rev. B **110**, 075154 (2024).

[23] P. Thalmeier, A. Akbari, and B. Schmidt, Thermodynamics, elastic anomalies and excitations in the field induced phases of $CeRh_2As_2$, New J. Phys. **27**, 033026 (2025).

[24] P. Khanenko, D. Hafner, K. Semeniuk, J. Banda, T. Lühmann, F. Bärtl, T. Kotte, J. Wosnitza, G. Zwicknagl, C. Geibel, J. F. Landaeta, S. Khim, E. Hassinger, and M. Brando, Origin of the non-Fermi-liquid behavior in $CeRh_2As_2$, Phys. Rev. B **111**, 045162 (2025).

[25] A. Amin, H. Wu, T. Shishidou, and D. F. Agterberg, Kramers' degenerate magnetism and superconductivity, Phys. Rev. B **109**, 024502 (2024).

[26] A. L. Szabó and A. Ramires, Superconductivity-induced improper orders in nonsymmorphic systems, Phys. Rev. B **110**, L180503 (2024).

[27] C. Lee, D. F. Agterberg, and P. M. R. Brydon, Unified picture of superconductivity and magnetism in $CeRh_2As_2$, Phys. Rev. Lett. **135**, 026003 (2025).

[28] H. Siddiquee, Z. Rehfuss, C. Broyles, and S. Ran, Pressure dependence of superconductivity in $CeRh_2As_2$, Phys. Rev. B **108**, L020504 (2023).

[29] K. Semeniuk, M. Pfeiffer, J. F. Landaeta, M. Nicklas, C. Geibel, M. Brando, S. Khim, and E. Hassinger, Exposing the odd-parity superconductivity in $CeRh_2As_2$ with hydrostatic pressure, Phys. Rev. B **110**, L100504 (2024).

[30] M. Pfeiffer, K. Semeniuk, J. F. Landaeta, R. Borth, C. Geibel, M. Nicklas, M. Brando, S. Khim, and E. Hassinger, Pressure-tuned quantum criticality in the locally noncentrosymmetric superconductor $CeRh_2As_2$, Phys. Rev. Lett. **133**, 126506 (2024).

[31] L. Akselrud and Y. Grin, WinCSD: Software package for crystallographic calculations (version 4), J. Appl. Cryst. **47**, 803 (2014).

[32] F. C. Ragel, P. D. V. du Plessis, and A. M. Strydom, Effects of La dilution on the $CePt_2Si_2$ Kondo lattice, J. Phys.: Condens. Matter **20**, 055218 (2008).

[33] Y. Ōnuki, T. Hirai, T. Kumazawa, T. Komatsubara, and Y. Oda, Heavy fermion state and superconductivity in $Ce_xLa_{1-x}Cu_2Si_2$, J. Phys. Soc. Jpn. **56**, 1454 (1987).

[34] B. Andraka, C. Jee, J. Kim, H. Li, M. Meisel, and G. Stewart, Heavy-fermion, magnetic and superconducting behavior of (Ce, M)Cu_2Si_2; $M = Y$, La, Th, Physica B **171**, 384 (1991).

[35] M. Očko, D. Drobac, B. Buschinger, C. Geibel, and F. Steglich, Transport properties of the $Ce_xLa_{1-x}Cu_{2.05}Si_2$ heavy-fermion alloy system, Phys. Rev. B **64**, 195106 (2001).

[36] C. Petrovic, S. L. Bud'ko, V. G. Kogan, and P. C. Canfield, Effects of La substitution on the superconducting state of $CeCoIn_5$, Phys. Rev. B **66**, 054534 (2002).

[37] J. F. Landaeta, A. M. León, S. Zwickel, T. Lühmann, M. Brando, C. Geibel, E.-O. Eljaouhari, H. Rosner, G. Zwicknagl, E. Hassinger, and S. Khim, Conventional type-II superconductivity in locally noncentrosymmetric $LaRh_2As_2$ single crystals, Phys. Rev. B **106**, 014506 (2022).

[38] See Supplemental Material at http://link.aps.org/supplemental/10.1103/f79y-ssdx for a detailed description of the data analyses, which include Refs. [49–55].

[39] M. L. Ali, M. K. Alam, M. Khan, M. N. M. Nobin, N. Islam, U. Faruk, and M. Z. Rahaman, Pressure-dependent structural, electronic, optical, and mechanical properties of superconductor $CeRh_2As_2$: A first-principles study, Physica B **668**, 415224 (2023).

[40] U. Ahlheim, M. Winkelmann, P. van Aken, C. Bredl, F. Steglich, and G. Stewart, Pair breaking in the heavy-fermion superconductors $Ce_{1-x}M_xCu_{2.2}Si_2$ and $U_{1-x}M_xBe_{13}$ (M = Th, La, Y and Gd), J. Magn. Magn. Mater. **76–77**, 520 (1988).

[41] F. Steglich, U. Ahlheim, U. Rauchschwalbe, and H. Spille, Heavy fermions and superconductivity: "Superconducting spectroscopy" of non-magnetic impurities in $CeCu_2Si_2$, Physica B+C **148**, 6 (1987).

[42] A. A. Abrikosov and L. P. Gor'kov, Contribution to the theory of superconducting alloys with paramagnetic impurities, Zh. Eksp. Teor. Fiz. **39**, 1781 (1960), [Sov. Phys. JETP **12**, 1243 (1961)].

[43] L. A. Openov, Critical temperature of an anisotropic superconductor containing both nonmagnetic and magnetic impurities, Phys. Rev. B **58**, 9468 (1998).

[44] T. Chen, H. Siddiquee, Q. Xu, Z. Rehfuss, S. Gao, C. Lygouras, J. Drouin, V. Morano, K. E. Avers, C. J. Schmitt, A. Podlesnyak, J. Paglione, S. Ran, Y. Song, and C. Broholm, Quasi-two-dimensional antiferromagnetic spin fluctuations in the spin-triplet superconductor candidate $CeRh_2As_2$, Phys. Rev. Lett. **133**, 266505 (2024).

[45] Y. Wu, Y. Zhang, S. Ju, Y. Hu, Y. Huang, Y. Zhang, H. Zhang, H. Zheng, G. Yang, E.-O. Eljaouhari, B. Song, N. C. Plumb, F. Steglich, M. Shi, G. Zwicknagl, C. Cao, H. Yuan, and Y. Liu, Fermi surface nesting with heavy quasiparticles in the locally noncentrosymmetric superconductor $CeRh_2As_2$, Chin. Phys. Lett. **41**, 097403 (2024).

[46] B. Chen, H. Liu, Q.-Y. Wu, C. Zhang, X.-Q. Ye, Y.-Z. Zhao, J.-J. Song, X.-Y. Tian, B.-L. Tan, Z.-T. Liu, M. Ye, Z.-H. Chen, Y.-B. Huang, D.-W. Shen, Y.-H. Yuan, J. He, Y.-X. Duan, and J.-Q. Meng, Exploring possible Fermi surface nesting and the nature of heavy quasiparticles in the spin-triplet superconductor candidate $CeRh_2As_2$, Phys. Rev. B **110**, L041120 (2024).

[47] X. Chen, L. Wang, J. Ishizuka, R. Zhang, K. Nogaki, Y. Cheng, F. Yang, Z. Chen, F. Zhu, Z. Liu, J. Mei, Y. Yanase, B. Lv, and Y. Huang, Coexistence of near-E_F flat band and van Hove singularity in a two-phase superconductor, Phys. Rev. X **14**, 021048 (2024).

[48] S. L. Ravi Sankar, Data for the manuscript titled: "La substitution studies on the heavy-fermion superconductor $CeRh_2As_2$", Edmond (2026), https://doi.org/10.17617/3.HMFH1A.

[49] N. W. Ashcroft and N. D. Mermin, *Solid State Physics* (Holt, Rinehart and Winston, New York, 1976).

[50] R. J. Radtke, K. Levin, H.-B. Schüttler, and M. R. Norman, Predictions for impurity-induced T_c suppression in the high-temperature superconductors, Phys. Rev. B **48**, 653(R) (1993).

[51] A. Ranna, R. Grasset, M. Gonzalez, K. Lee, B. Y. Wang, E. Abarca Morales, F. Theuss, Z. H. Filipiak, M. Moravec, M. Konczykowski, H. Y. Hwang, A. P. Mackenzie, and B. H. Goodge, Disorder-induced suppression of superconductivity in infinite-layer nickelates, Phys. Rev. Lett. **135**, 126501 (2025).

[52] M. T. Hutchings, Point-charge calculations of energy levels of magnetic ions in crystalline electric fields, Solid State Phys. **16**, 227 (1964).

[53] K. W. H. Stevens, Matrix elements and operator equivalents connected with the magnetic properties of rare earth ions, Proc. Phys. Soc. A **65**, 209 (1952).

[54] F. Marabelli, P. Wachter, and J. Franse, Electronic structure of UPt_3: A low energy optical study, J. Magn. Magn. Mater. **62**, 287 (1986).

[55] F. Marabelli and P. Wachter, Temperature dependence of the optical conductivity of the heavy-fermion system $CeCu_6$, Phys. Rev. B **42**, 3307 (1990).